

Characterization of the zwitterionic intermediate in 1,1-carbaboration of alkynes

Alessandro Bismuto,^[a] Gary S. Nichol,^[a] Fernanda Duarte,^{[b]*} Michael J. Cowley,^{[a]*} Stephen P. Thomas^{[a]*}

^[a] Dr A. Bismuto, Dr G. S. Nichol, Dr M.J. Cowley, Dr S. P. Thomas

^aEaStCHEM, School of Chemistry, University of Edinburgh, Joseph Black Building, David Brewster Road, Edinburgh, EH9 3FJ.
E-mail: Michael.Cowley@ed.ac.uk, Stephen.Thomas@ed.ac.uk

^[b] Dr F. Duarte

^bChemistry Research Laboratory, University of Oxford, 12 Mansfield Road, Oxford, OX1 3TA, UK
E-mail: Fernanda.DuarteGonzalez@chem.ox.ac.uk

Experimental procedure and DFT coordinates provided via the link in the Supporting information.

Abstract: The reaction of a Lewis acidic borane with an alkyne is a key step in a diverse range of main group transformations. Alkyne 1,1-carbaboration, the Wrackmeyer reaction, is an archetypal transformation of this kind. 1,1-Carbaboration has been proposed to proceed through a zwitterionic intermediate. We report the isolation and spectroscopic, structural and computational characterization of the zwitterionic intermediates generated by reaction of $B(C_6F_5)_3$ with alkynes. The stepwise reactivity of the zwitterion provides new mechanistic insight for 1,1-carbaboration and wider $B(C_6F_5)_3$ catalysis. Making use of intramolecular stabilization by a ferrocene substituent, we have characterized the zwitterionic intermediate in the solid state and diverted reactivity towards alkyne cyclotrimerization.

The use of main group species has garnered significant interest as sustainable catalysis alternatives.^[1] Lewis acidic boranes, particularly tris(pentafluorophenyl)borane ($B(C_6F_5)_3$), have been extensively investigated and the reaction of $B(C_6F_5)_3$ and related boranes, with an alkyne is key to a number of reactivity pathways including frustrated Lewis pair chemistry^[2] and the Wrackmeyer reaction^[3,4] (Scheme 1, A).

1,1-Carbaboration was first reported by Wrackmeyer using silyl- or stannyl-substituted alkynes.^[3,4] The substrate scope was significantly expanded using strongly Lewis acidic boranes (Scheme 1, B).^[5,6] Computational studies suggest that 1,1-carbaboration using $B(C_6F_5)_3$ proceeds by alkyne coordination to $B(C_6F_5)_3$ to form a zwitterion **I**, a σ -adduct of the alkyne and $B(C_6F_5)_3$.^[7-9] 1,2-Hydride shift (Scheme 1, B; $R^2 = H$) and aryl migration from boron to carbon gives the alkenyl borane. Direct experimental evidence for this mechanism is scant; only tentative evidence from NMR spectroscopy for the zwitterionic intermediate **I** has been reported.^[10]

$B(C_6F_5)_3$ is by far the most widely used acid component in FLPs, enabling the synergistic activation of small molecules and unsaturated bonds.^[2] Stephan^[11] and Erker,^[7,12] reported the reactivity of alkynes towards $B(C_6F_5)_3$ /phosphine FLPs, which result in the apparent trapping of the σ -adduct **I** by the Lewis base.^[12b]

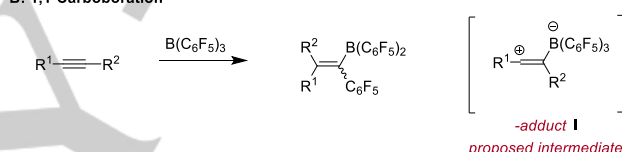
Here, we report the isolation and full spectroscopic and structural characterization of the zwitterionic intermediate in $B(C_6F_5)_3$ -mediated 1,1-carbaboration.

A: Reactions with Alkynes

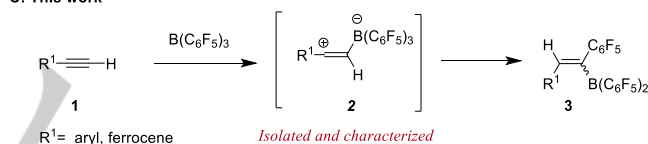
Wrackmeyer reaction



B: 1,1-Carbaboration



C: This work



Scheme 1. A) Wrackmeyer reaction and FLP chemistry; B) 1,1-Carbaboration of alkynes. C) This work.

We began by examining the stoichiometric reaction of phenylacetylene and $B(C_6F_5)_3$. Rapid combination of phenylacetylene and one equivalent of $B(C_6F_5)_3$ in toluene- d_8 at 195 K produced an intensely red solution.^[13] On warming to 233 K, a new signal in the 1H NMR spectrum at δ 5.41 was observed, which was attributed to the alkenyl proton of the zwitterion **2a**. $^{13}C\{^1H\}$ NMR revealed a distinctive downfield signal at δ 199.3, typical of alkenyl-cations.^[14] A 1H - ^{13}C HMBC experiment showed a correlation between these two signals (Figure S1). The expected high-field chemical shift for the four-coordinate boron center was observed at δ -12.1 in the ^{11}B NMR spectrum, which correlated with the alkenyl proton by 1H - ^{11}B HMBC. Using ^{13}C -labelled ($PhC\equiv^{13}CH$), we observed a quartet at δ 51.2 by ^{13}C NMR spectroscopy, assigned as the boron-coordinated C1 of the zwitterion **2a** ($^1J_{B-C} = 44$ Hz). A corresponding doublet (δ -12.1, $^1J_{B-C} = 44$ Hz) was observed in the ^{11}B NMR spectrum (Figure 1). A DEPT 135 ^{13}C NMR spectrum confirmed the signal at δ 199.3 was C2 (Figures S2 and S3).^[13] Even at 233 K, significant quantities of unreacted phenylacetylene and $B(C_6F_5)_3$ remain, indicating that the zwitterion **2a** may exist in equilibrium with the

COMMUNICATION

starting materials. Upon warming above 243 K, rearrangement to the 1,1-carboboration product **3a** was observed,^[8] alongside unidentified side products.

With solution-state evidence for intermediate **2a**, we sought a more stable analogue. We rationalized that an electron-donating substituent would improve the zwitterion stability. Reaction of *p*-methoxy phenylacetylene with B(C₆F₅)₃ immediately gave the characteristic resonances of a zwitterionic intermediate **2b**, as observed by ¹H, ¹³C, and ¹¹B NMR spectroscopy (Figure 1B and S4). Intermediate **2b** was more stable than the unsubstituted analogue with no 1,1-carboboration observed below room temperature, and the zwitterion **2b** persisted for up to 2 days at room temperature. The ¹³C chemical shifts of the two-coordinate C2 centers of **2a** and **2b** (**2a** δ 199.3; **2b** δ 193.5) are typical for alkenyl-cations,^[14a-c] and the lower chemical shift of the methoxy-substituted zwitterion **2b** is consistent with the presence of the more strongly electron-donating substituent.

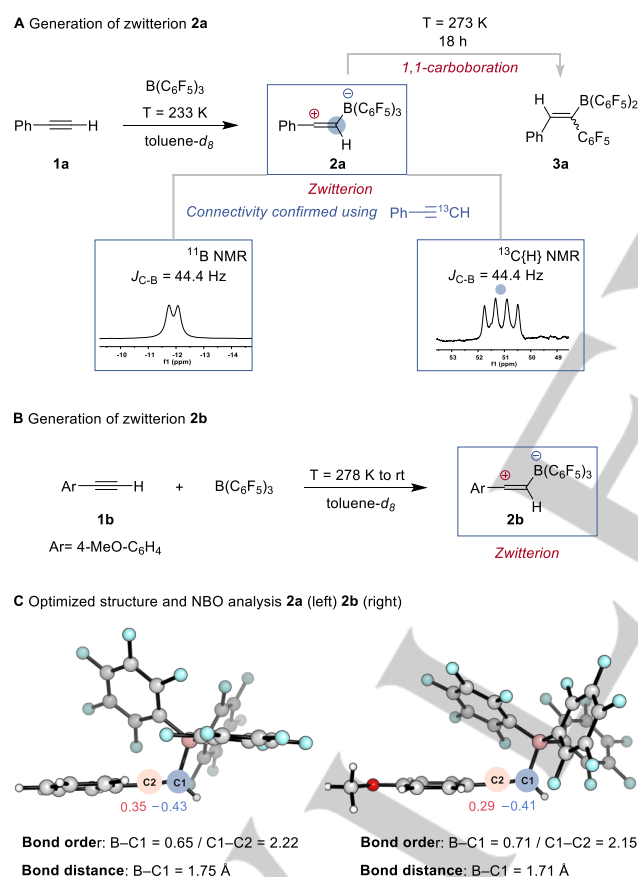
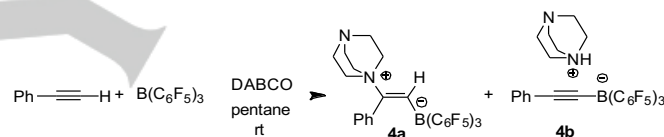


Figure 1. A) Reaction conditions and NMR spectroscopy for the generation of **2a**. B) Conditions for the generation of **2b**. C) Optimized structures, NPA charges (red/blue text), and Wiberg bond orders for **2a** and **2b**. Geometry optimizations and NBO calculations were carried out at the SMD[toluene]-PBED3BJ/6-31G* and SMD[toluene]-M06-2X/6-311+G**/SMD[toluene]-PBED3BJ/6-31G* levels of theory, respectively).

The formation of **2a** has previously been predicted on the basis of density functional theory (DFT) calculations.^[7-9] To gain additional insights into the structure of **2a** and **2b**, DFT calculations (SMD[toluene]-M06-2X/6-311+G**/SMD[toluene]-

PBED3BJ/6-31G*) were performed. Both species were found to be stable minima and slightly higher in energy than the starting materials (8.5 and 4.0 kcal mol⁻¹, respectively), consistent with previous work (Figure 1C).^[7-9] A transition state connecting **2a** and **2b** to the experimentally observed 1,1-carboboration products was also obtained (Figure S5). NBO analysis revealed the expected decreased C–C Wiberg bond orders in **2a** and **2b** when compared to the free alkynes (**2a**: 2.22; **2b**: 2.15). The observed B–C bond order increased with the addition of the *para*-OMe group of **2b** (**2a**: 0.65; **2b**: 0.71). Correspondingly, the B–C bond distance in **2a** was longer than that in **2b** (1.75 vs 1.71 Å). NPA analysis reveals significant build-up of positive charge at the two-coordinate carbon center C2, confirming the cationic character (Figure 1C, NPA charges, **2a**: 0.35; **2b**: 0.29).

Phosphine, amine and B(C₆F₅)₃ FLPs have been reported to activate alkynes to 1,2-addition of the Lewis acid and base to form zwitterionic borates.^[2a,11] Stephan speculated that the mechanism of this reaction involved an initial π -interaction of the alkyne with B(C₆F₅)₃ which enabled nucleophilic attack of the amine/phosphine. Consistent with previous findings, generation of the zwitterion in the presence of Lewis base 1,4-diazabicyclo[2.2.2]octane (DABCO) gave a mixture of the trapped adducts **4a** and **4b** (50% combined yield after 24 h). Solution phase characterization of the DABCO adducts **4a** and **4b** showed they exist in equilibrium.^[7] Consistent with this, isolated acid-base pair **4b** slowly converted to a mixture of adduct **4a** and acid-base pair **4b** in CD₂Cl₂ (Figure S7).



Scheme 2. Trapping DABCO adduct **4**.

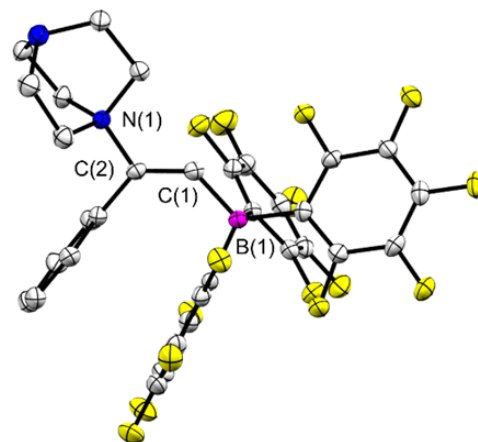
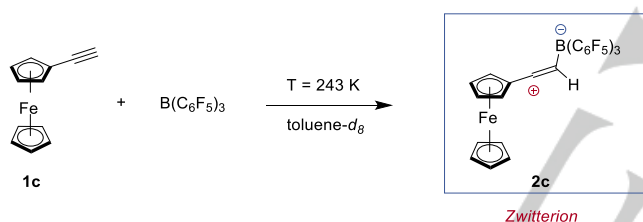


Figure 2. Crystal Structure of the zwitterion (**4a**). Ellipsoids are set to 50% probability; hydrogen atoms are omitted for clarity. Selected bond lengths (Å) and angles [°]: B(1)–C(1) 1.630(4), C(1)–C(2) 1.324(4), N(1)–C(2) 1.534(3); B(1)–C(1)–C(2) 128.4(2), C(1)–C(2)–N(1) 121.1(2).

Although the NMR spectroscopic evidence for the formation of zwitterions **2a** and **2b** was convincing, we were unable to isolate single crystals of these species. Ferrocenyl substituents have been used to stabilize carbocations^[15-17] and silyl cations.^[18-20] Furthermore, short-lived alkenyl cations have been characterized by NMR spectroscopy.^[21] We therefore postulated that a zwitterion generated from ethynyl ferrocene and B(C₆F₅)₃ may be stable.

COMMUNICATION

Ethynylferrocene was reacted with $\text{B}(\text{C}_6\text{F}_5)_3$ at 243 K, and the reaction monitored by NMR spectroscopy. Consumption of the starting materials and formation of the zwitterionic alkenyl cation **2c** was observed as the major initial product (see later) by ^1H NMR spectrum (Scheme 3). The alkenyl proton was assigned to a resonance at δ 6.92, which correlated with signals in the ^{13}C NMR spectrum at δ 107.8 and 186.7 in HSQC and HMBC experiments. The signal at δ 107.8 was assigned to the three-coordinate alkenyl carbon bound to boron. The signal at δ 186.7 was assigned to the cationic carbon (Figure S8). Although at much higher field than the signals observed for the phenylacetylene or methoxyphenylacetylene adducts **2a** and **2b**, the chemical shift is consistent with previously reported ferrocenyl alkenyl cations^[15–17] and potentially indicates a stabilizing interaction with the iron center. Unusually, no ^1H - ^{11}B or ^{11}B - ^{13}C coupling was observed, even when 2- ^{13}C -ethynylferrocene was used. However, the ^{13}C -labelled ethynylferrocene enabled the measurement of the ^{13}C - ^{13}C coupling constant in the alkenyl unit of the zwitterion **2c** ($^1J_{\text{C-C}} = 99$ Hz), which was substantially decreased compared to the alkyne starting material ($^1J_{\text{C-C}} = 177$ Hz). This decrease is consistent with the lower C–C bond order and a change in hybridization from sp to sp^2 . Similarly the $^1J_{\text{C-H}}$ coupling constant was observed to fall from 250 Hz in the alkyne **1c** to 165 Hz in zwitterion **2c** (Figure S9). Single crystals of zwitterion **2c** suitable for X-ray diffraction were grown from the reaction mixture at low temperature (Figure 3) and confirmed the proposed zwitterionic structure.



Scheme 3. Reaction of $\text{B}(\text{C}_6\text{F}_5)_3$ and ethynylphenylacetylene

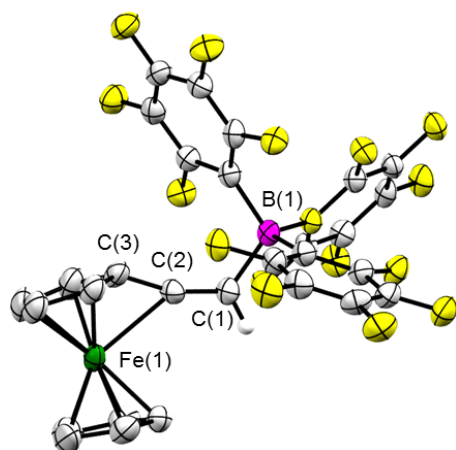


Figure 3. Crystal Structure of the alkenyl ferrocene zwitterion (**2c**). Ellipsoids are set to 50% probability; hydrogen atoms are omitted for clarity with the exception of the alkenyl C–H bond. Selected bond lengths (Å) and angles [$^\circ$]: B(1)–C(1) 1.654(5), C(1)–C(2) 1.286(5), C(2)–C(3) 1.379(5), Fe(1)–C(2) 2.379(4), Fe(1)–C(2) 1.990(4); B(1)–C(1)–C(2) 122.8(3), Fe(1)–C(2)–C(1)–140.47(2), C(3)–C(2)–C(1) 162.6(4).

A significant distortion of the geometry around the alkenyl unit was observed in the solid-state indicating significant stabilization from the iron center. The C–C bond distance in the alkenyl unit was

1.286(5) Å, significantly longer than that observed for ethynylferrocene (1.17(3) Å),^[22] comparable to that of the DABCO adduct **4a** (1.324(4) Å), and consistent with a reduction in bond order and the observed reduction in $^1J_{\text{C-C}}$ coupling. The three coordinate C1 adopts the expected trigonal planar geometry (sum of angles at C1 = 360.0(3) $^\circ$) and the B1–C1 bond distance is 1.654(5) Å, also comparable to that in **4a** (1.630(4) Å).

The relatively short C(3)–C(2) bond length (1.379(5) Å) and the Fe(1)–C(2) distance (2.379(4) Å) indicate some charge delocalization to the ferrocene motif. Consistent with this, the tilt angle of the Cp rings in the ferrocene unit is 11.13(4) $^\circ$. The dip angle of the alkenyl substituent from its Cp ring, α^* , is 36.1(4) $^\circ$, which is significantly greater than that reported for the diphenylferrocenylcarbenium ion, and begins to approach those reported for ferrocenylsilylium ions.^[16,18] The large dip angle results in the short Fe1–C2 bond distance (2.379(4) Å), again substantially less than in ferrocenylcarbenium ion (2.715(6) Å). The short Fe1–C2 distance and large dip angle of **2c** are close to those calculated for the parent ferrocenylcarbenium ion,^[23] consistent with the reduced steric and increased electronic demand at the cationic carbon compared to diphenylferrocenylcarbenium. The structural features of the ferrocene-substituted zwitterion **2c** strongly suggest stabilization of the carbocationic center through an interaction with iron.

DFT calculations were used to better understand the unusual bonding of **2c**. Calculations with the popular M06-2X functional led to a geometry substantially different to the one obtained experimentally. Geometry optimization was repeated with a range of DFT functionals and compared to the X-ray model (Figure 4A, figure S10). Among them, the computationally less expensive PBE-D3BJ best reproduced the solid-state structure of **2c** (root mean square deviation (rmsd) = 0.23 vs 0.48 Å for M06-2X). There was significant bonding character in the iron–C2 interaction, as apparent from the calculated Wiberg bond order of 0.16. The C1–C2 bond order was reduced from 2.84 in the alkyne precursor to 2.09, whilst the C2–C3 (Cp ipso) bond has a degree of multiple bond character with a bond order of 1.28 (Figure 4B, S11). These bond orders, together with the observed bond-length alternation in the substituted Cp ring indicate a degree of allenic character to the C1–C2–C3 unit. The donor–acceptor character of the C1–B1 bond is apparent from the accumulation of negative charge at C1 (NPA charge –0.43) and the reduced C1–B1 bond order of 0.73, as well as the heavy polarisation towards C2 (67% C, 33% B). Calculated NMR chemical shifts of **2a–2c**, followed the experimental trends (Figure S12).

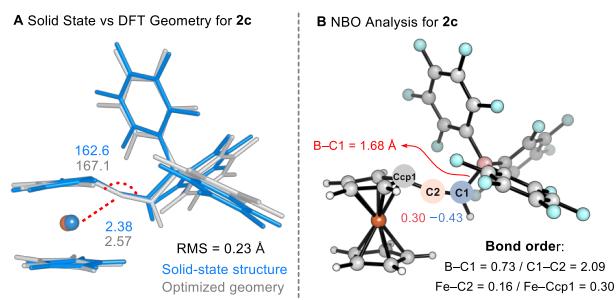


Figure 4. A) comparison of solid-state structure and optimized structure of **2c** at the SMD[toluene]-PBE-D3BJ/6-31G*/SDD (Fe) level of theory. B) NBO analysis of **2c** at the SMD[toluene]-M06-2X/6-311+G**/SMD[toluene]-PBE-D3BJ/6-31G* level of theory.

COMMUNICATION

Although solutions of the simple aryl substituted zwitterions **2a** and **2b** were observed to progress to 1,1-carbaboration products (Figure 1 and Scheme 2), the fate of ferrocenyl substituted zwitterion **2c** was more complex. Reactions of ethynylferrocene and $B(C_6F_5)_3$ at 243 K showed complete consumption of the starting materials and formation of zwitterion **2c**. Upon warming to room temperature complex mixtures of products were obtained without any 1,1-carbaboration products. In one case we were able to obtain a small quantity of product sufficient for a single-crystal X-ray diffraction analysis, with the compound obtained proving to be the result of a complex trimerization/multiple carboboration reaction to give bicycle **5**. We tentatively propose that this unique product arises as a result of the longer lifetime of the stabilized ferrocenyl zwitterion **2c** introducing a Lewis acid of similar potency to $B(C_6F_5)_3$, and thus sequestering additional alkyne units. Inter- and, subsequent, intramolecular reaction of ethynylferrocene with the zwitterion **2c**, and concurrent 1,1- and 1,4-carbaboration, lead to the cyclopropylcyclohexene **5** from a single $B(C_6F_5)_3$ and three alkyne units.^[24]

In summary, we have observed, characterized and trapped the proposed zwitterionic intermediates in 1,1-carbaboration reactions. We have shown that these intermediates, like carbenium ions, can be stabilized by interactions with a ferrocene substituent, resulting in increased lifetimes and changes to reactivity patterns. We are currently investigating the role of *in situ* generated alkenyl zwitterions in catalysis and investigating the mechanism of the formation of **5**.

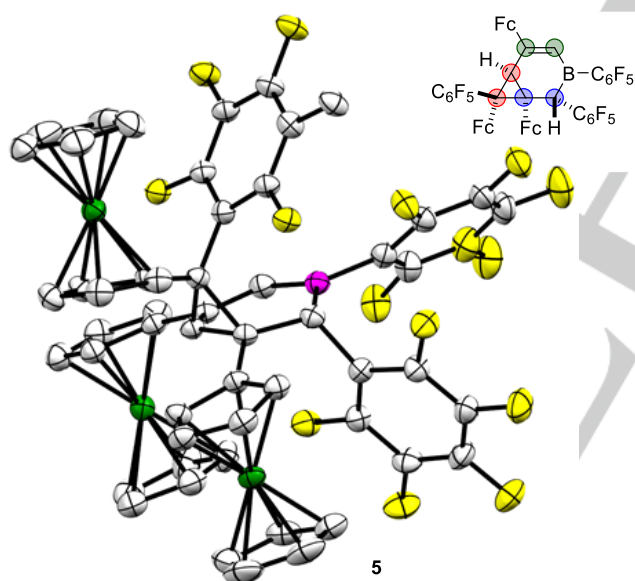


Figure 5. Crystal Structure of the cyclootrimerization product (**5**). Ellipsoids are set to 50% probability; hydrogen atoms are omitted for clarity. Selected bond lengths (Å): B(1)–C(1) 1.609(5), B(1)–C(5) 1.507(5), C(1)–C(2) 1.527(4), C(2)–C(3) 1.523(4), C(3)–C(4) 1.483(4), C(4)–C(5) 1.372(4), C(2)–C(6) 1.564(4), C(3)–C(6) 1.538(4). Fc = Ferrocenyl, \circ = alkyne units.

Acknowledgements

MJC and SPT thank the University of Edinburgh for funding. SPT thanks the Royal Society for a URF. All thank the EPSRC and CRITICAT CDT for financial support (EP/L016419/1). All thank Mr.

Juraj Bella for NMR technical advice, and Dr Martin Stanford for fruitful discussions. F.D. thanks the EPSRC Tier-2 National HPC Facility Service (<http://www.cirrus.ac.uk>), and the EPSRC Centre for Doctoral Training for Theory and Modelling in Chemical Sciences (EP/L015722/1) for providing access to the Dirac cluster at Oxford.

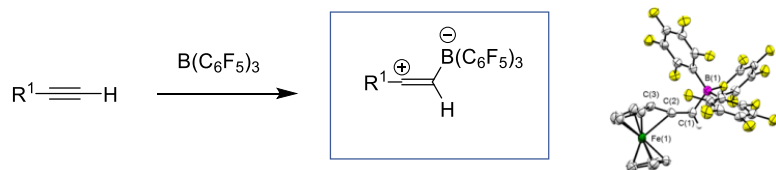
Keywords: 1,1-carbaboration • vinyl cation • mechanistic investigation • FLP

- [1] For references about main group reactivity see: a) P. P. Power, *Nature* **2010**, 463, 171–177; b) T. A. Engesser, M. R. Lichtenthaler, M. Schleep, I. Krossing, *Chem. Soc. Rev.* **2016**, 45, 789–899. c) R. L. Melen, *Science* **2019**, 363, 479–484; d) J. R. Lawson, R. L. Melen, *Inorg. Chem.* **2017**, 56, 8627–8643.
- [2] For relevant reviews about FLP chemistry see: a) D. W. Stephan, *J. Am. Chem. Soc.* **2015**, 137, 10018–10032; b) D. W. Stephan, G. Erker, *Angew. Chem. Int. Ed.* **2015**, 54, 6400–6441; c) D. W. Stephan, *Acc. Chem. Res.* **2015**, 48, 306–316; d) J. Paradies, *Coord. Chem. Rev.* **2019**, 380, 170–183; e) J. Lam, K. M. Szkop, E. Mosafari, D. W. Stephan, *Chem. Soc. Rev.* **2019**, 48, 3592–3612.
- [3] B. Wrackmeyer, K. Horchler, R. Boese, *Angew. Chem. Int. Ed.* **1989**, 28, 1500–1502.
- [4] a) B. Wrackmeyer, *Coord. Chem. Rev.* **1995**, 145, 125–156; b) B. Wrackmeyer, S. Bayer, W. Milius, E. V. Klimkina, *J. Organomet. Chem.* **2018**, 865, 80–88.
- [5] a) G. Kehr, G. Erker, *Chem. Commun.* **2012**, 48, 1839–1850.
- [6] a) C. Chen, T. Voss, R. Fröhlich, G. Kehr, G. Erker, *Org. Lett.* **2011**, 13, 62–65; b) C. Fan, W. E. Piers, M. Parvez, R. McDonald, *Organometallics* **2010**, 29, 5132–5139; c) K. Škoch, C. Pauly, C. G. Daniliuc, K. Bergander, G. Kehr, G. Erker, *Dalt. Trans.* **2019**, 48, 4837–4845.
- [7] C. Chen, F. Eweiner, B. Wibbeling, R. Fröhlich, S. Senda, Y. Ohki, K. Tatsumi, S. Grimme, G. Kehr, G. Erker, *Chem. An Asian J.* **2010**, 5, 2199–2208.
- [8] C. Jiang, O. Blacque, H. Berke, *Organometallics* **2010**, 29, 125–133.
- [9] R. Liedtke, R. Fröhlich, G. Kehr, G. Erker, *Organometallics* **2011**, 30, 5222–5232.
- [10] W. Nie, G. Sun, C. Tian, M. V. Borzov, *Zeitschrift für Naturforsch. B* **2016**, 71, 1029–1041.
- [11] a) M. A. Dureen, D. W. Stephan, *J. Am. Chem. Soc.* **2009**, 131, 8396–8397; b) M. A. Dureen, C. C. Brown, D. W. Stephan, *Organometallics* **2010**, 29, 6594–6607; c) J. S. Reddy, B. H. Xu, T. Mahdi, R. Fröhlich, G. Kehr, D. W. Stephan, G. Erker, *Organometallics* **2012**, 31, 5638–5649; d) R. L. Melen, M. M. Hansmann, A. J. Lough, A. S. K. Hashmi, D. W. Stephan, *Chem. Eur. J.* **2013**, 19, 11928–11938; e) K. Chernichenko, Á. Madarász, I. Pápai, M. Nieger, M. Leskelä, T. Repo, *Nat. Chem.* **2013**, 5, 718–723.
- [12] a) T. Wang, C. G. Daniliuc, C. Mück-Lichtenfeld, G. Kehr, G. Erker, *J. Am. Chem. Soc.* **2018**, 140, 3635–3643; b) P. Vasko, I. A. Zulkifly, M. Á. Fuentes, Z. Mo, J. Hicks, P. C. J. Kamer, S. Aldridge, *Chem. Eur. J.* **2018**, 24, 10531–10540.
- [13] The observation of the red solution and the 1H and ^{11}B chemical shifts that we observe for **2a** are consistent with those reported in reference 10.
- [14] a) Z. Rappoport, P. J. Stang, *Eds. Wiley: New York*, **1997**; b) T. Müller, M. Juhasz, C. A. Reed, *Angew. Chem. Int. Ed.* **2004**, 43, 1543–1546; c) P. A. Byrne, S. Kobayashi, E. U. Würthwein, J. Ammer, H. Mayr, *J. Am. Chem. Soc.* **2017**, 139, 1499–1511.
- [15] R. L. Sime, R. J. Sime, *J. Am. Chem. Soc.* **1974**, 96, 892–896.
- [16] U. Behrens, *J. Organomet. Chem.* **1979**, 182, 89–98.
- [17] A. Z. Kreindlin, M. I. Rybinskaya, *Russ. Chem. Rev.* **2004**, 73, 417–432.
- [18] K. Mütter, R. Fröhlich, C. Mück-Lichtenfeld, S. Grimme, M. Oestreich, M. J. Am. Chem. Soc. **2011**, 133, 12442–12444.
- [19] K. Mütter, P. Hrobárik, V. Hrobáriková, M. Kaupp, M. Oestreich, *Chem. A Eur. J.* **2013**, 19, 16579–16594.
- [20] A. R. Nödling, K. Mütter, V. H. G. Rohde, G. Hilt, M. Oestreich, *Organometallics* **2014**, 33, 302–308.

COMMUNICATION

- [21] a) E.-W. Koch, H.-U. Siehl and M. Hanack, *Tetrahedron Lett.*, **1985**, 26, 1493–1496. b) For examples of alkynyl/alkenyl boranes and phosphines derived from ethynylferrocene see; Z. Yuan, N. J. Taylor, Y. Sun, T. B. Marder, I. D. Williams, C. Lap-Tak, *J. Organomet. Chem.* **1993**, 449, 27–37.
- [22] K. Wurst, O. Elsner, H. Schottenberger, *Synlett* **1995**, 833–834.
- [23] C. Bleiholder, F. Rominger, R. Gleiter, *Organometallics*, **2009**, 28, 1014–1017.
- [24] a) M. M. Hansmann, R. L. Melen, F. Rominger, A. S. K. Hashmi, D. W. Stephan, *J. Am. Chem. Soc.* **2014**, 136, 777–782; b) M. A. Dureen, D. W. Stephan, *J. Am. Chem. Soc.* **2009**, 131, 8396–8397.

Entry for the Table of Contents



Observed and characterized by NMR, X-ray and DFT

We describe the isolation and the characterization of the zwitterionic intermediate in 1,1-carbaboration reactions. The highly reactive zwitterionic intermediates are generated from tris(pentafluorophenyl)borane and alkynes under reaction conditions of 1,1-carbaboration.

Twitter usernames: @AlexBismuto @cowley_group @SPTThomasGroup